Collision-induced Lamb dips in laser Stark spectroscopy*

J. W. C. Johns, A. R. W. McKellar, T. Oka, and M. Römheld†

Division of Physics, National Research Council of Canada, Ottawa, Ontario, Canada K1A 0R6
(Received 7 October 1974)

While observing inverse Lamb dips in infrared laser Stark spectra, we have found unexpected extra dips which lie midway between the "genuine" dips. These center dips are similar to those observed by Uzgiris, Hall, and Barger in that they are caused by a crossover of two different transitions due to the Doppler effect, but are different in that the two transitions do not share a common level. Thus these newly observed center dips are the result of a four-level infrared–infrared double resonance effect and they provide information on rotational transitions as well as on the velocity changes which occur during intermolecular collisions. Since the transitions which cause the center dips involve different M components of the same rotational level, this method is specially suited for the study of reorientation collisions, that is, collisions in which the direction of the total angular momentum changes without changing its magnitude. A theory is developed in which the relative intensities of the center dips with respect to those of "genuine" dips are related to the relative importance of reorientation collisions. The experiments were done on NH_3, H_2CO, and CH_3F using the CO and the CO_2 lasers. The following conclusions are obtained from analysis of the results: (a) The observation of sharp center dips confirms our previous conclusion (Ref. 3) that, as a result of weak collisions, rotational quantum states of molecules can change *without* appreciable change in velocity. (b) The variation of relative intensities for CH_3F, H_2CO, and NH_3 indicates that parity changing reorientation transitions are preferred to parity conserving transitions. (c) Analysis of very large signals for $J = K$ levels of CH_3F indicates that, for those levels, the rate of $\Delta M = \pm 1$ reorientation collisions relative to all inelastic collisions is of the order of 70%. The consideration of $\Delta M > 1$ transitions would further increase the relative importance of reorientation collisions. (d) Analysis of $\Delta M > 1$ signals in H_2CO indicates that rather large reorientations of molecules can occur during a single collision.

I. INTRODUCTION

In the last few years the selection rules which govern transitions between molecular rotational states induced by collisions have been investigated by the technique of microwave–microwave double resonance.[1] Recently the technique has been extended to infrared–microwave[2] and infrared–infrared[3,4] double resonance, and in the latter case it has been shown[3] that because of increased Doppler width in the infrared it is possible to monitor velocity changes as well as state changes due to collisions. In this paper, we report the observation of four-level infrared double resonance signals obtained during the course of studies using the technique of laser Stark Lamb dip spectroscopy.[5] Similar observations have recently been reported by Brewer, Shoemaker, and Stenholm.[6]

While observing inverse Lamb dips in the laser Stark spectrum of NH_3 using the CO laser, we found that when the dips are separated by less than the Doppler width, they are sometimes accompanied by extra dips which lie midway between the "genuine" dips.[7] Many similar "center dips" have also been observed in the Stark spectrum of CH_3F using the CO_2 laser.[8] These center dips are similar to previously observed[9] "crossover resonances" in that they lie midway between genuine dips and that they are caused, contrary to normal Lamb dips, by molecules with nonzero velocities along the direction of propagation of radiation (see Sec. II). However, when the energy level system involved in the observation was examined, we found an essential difference between the earlier case[9] and our present case. In the former, the two transitions responsible for the extra dips have one level in common and thus form a three-level system [Fig. 1(b)], whereas in the latter the two transitions are independent and thus form a four-level system [Fig. 1(c)]. In the four-level case, the connections between the two transitions are caused only by collisions and therefore, as stated in Ref. 8, we concluded that the center dips must be due to collisional transfer of molecules between levels. These collisions must involve very little change in the molecular velocities since the widths of the observed center dips are comparable to those of the original Lamb dips. The method provides a new way to observe four-level infrared double resonance and therefore to study simultaneously state changes and velocity changes due to collisions.

Since the initial observations, collision-induced center dips have been observed for virtually all the molecules which have been studied by the technique of laser Stark Lamb dip spectroscopy; they are CH_3F,[8] SiH_4,[10] CD_3F, and D_2CO in the 10 μm region, and NH_3[7] and H_2CO in the 5 μm region. In Sec. III a summary of the results so far obtained will be presented.

II. THEORY

A. Frequency matching

In a Lamb dip experiment, molecules are subjected to the oscillating fields of two radiations, one going in the positive direction along the z axis (denote this by E_+) and the other in the negative direction along the z axis (denoted E_-). The fields E_+ and E_- have the same frequency, ν_l, for laboratory observers, but molecules with a velocity component v along the z axis feel the frequencies of E_+ and E_- to be $\nu_l\,(1-v/c)$ and $\nu_l\,(1+v/c)$, respectively, due to the Doppler effect. Lamb dips are caused when molecules with a certain velocity component v are resonant for both E_+ and E_-.

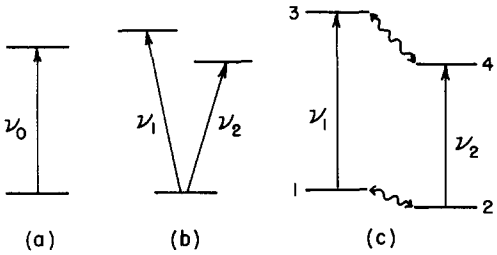

FIG. 1. Schematic energy level diagrams, illustrating (a) single resonance, (b) three-level double resonance, and (c) four-level double resonance. The wavy arrows in (c) represent collision-induced transitions.

In a two-level system [Fig. 1(a)], this occurs only when $\nu_l = \nu_0$ and $v = 0$, that is, only molecules with zero velocity component contribute to the signal. For a three-level system [Fig. 1(b)], however, in addition to the two normal Lamb dips corresponding to $\nu_l = \nu_1$ and $\nu_l = \nu_2$ with $v = 0$, the condition for an inverse Lamb dip is also met by a set of v and nonzero velocities v_m such that either

$$\nu_l(1 + v_m/c) = \nu_1 \text{ and } \nu_l(1 - v_m/c) = \nu_2$$

or

$$\nu_l(1 + v_m/c) = \nu_2 \text{ and } \nu_l(1 - v_m/c) = \nu_1 \quad , \tag{1}$$

that is, the oscillating fields E_+ and E_- affect molecules with the same velocity v_m by means of different transitions. This causes the center dips observed by Uzgiris *et al.*[9] at the frequency and velocity

$$\nu_l = (\nu_1 + \nu_2)/2$$

and

$$v_m = \pm c(\nu_1 - \nu_2)/2\nu_l \neq 0 \quad . \tag{2}$$

It is seen that the extra dip appears midway between the two normal dips and that, because of the Maxwellian molecular velocity distribution, they are not observable when $\nu_1 - \nu_2$ is much greater than twice the Doppler width. Molecules with two velocity components contribute to this phenomenon. A detailed theory for this three-level system has been worked out by Schlossberg and Javan.[11]

In a four-level system [Fig. 1(c)], the same expressions [Eqs. (1) and (2)] apply but, since the transitions are separate, the saturation of one transition affects the other only via collision-induced transitions between levels as indicated by wavy arrows in Fig. 1(c). This situation is new in our experiment and will be considered in detail in Sec. II B. However before considering collisions, we will modify Eqs. (1) and (2) according to our experimental arrangement. In Eqs. (1) and (2) it is assumed, for simplicity, that ν_1 and ν_2 are fixed molecular quantities and that the frequency of radiation ν_l is varied, as is the case when a tunable laser is used for observation. In our experiment, the frequency of radiation is fixed at the laser frequency ν_l and the transition frequencies $\nu_1(E)$ and $\nu_2(E)$ are varied by applying a static electric field E. The experimental arrangement is indicated in Fig. 2. More detailed descriptions of the apparatus are given elsewhere.[7,8,12] Using the laser Stark technique, the two normal Lamb dips are observed at the dc electric fields E_1 and E_2 which satisfy

$$\nu_1(E_1) = \nu_2(E_2) = \nu_l \quad . \tag{3}$$

The center dip occurs at a field E_m for which either

$$\nu_l(1 + v_m/c) = \nu_1(E_m) \text{ and } \nu_l(1 - v_m/c) = \nu_2(E_m)$$

or

$$\nu_l(1 + v_m/c) = \nu_2(E_m) \text{ and } \nu_l(1 - v_m/c) = \nu_1(E_m) \quad . \tag{4}$$

If the Stark shift is linear in electric field, as in CH_3F, and $\nu_i = \nu_i^0 + \alpha_i E$, E_m is expressed as

$$E_m = \tfrac{1}{2}(E_1 + E_2) + [(\alpha_1 - \alpha_2)/2(\alpha_1 + \alpha_2)](E_1 - E_2) \quad . \tag{5}$$

Since the second term in Eq. (5) is very small the extra dip appears almost exactly at the center. If the Stark shift is nonlinear as in NH_3, the extra dip will be off center in terms of electric field.

B. Collision-induced dips

In the experimental arrangement shown in Fig. 2, the radiation E_- is observed by the detector. In double resonance terminology, the oscillating field E_+ "pumps" molecules while the field E_- "monitors" the change due to pumping. Assuming that $\nu_1(E) > \nu_2(E)$ in the region of field of interest, $E \approx E_m$, we see that E_+ pumps the ν_2 transition and E_- monitors the ν_1 transition, or E_+ pumps the ν_1 transition and E_- monitors the ν_2 transition for positive v_m and negative v_m, respectively. We consider only the former case in detail because the treatment for the latter is similar.

Since the randomness of collisional processes interrupts the coherence of states, the problem can be dealt with simply by considering population changes in the levels. As is customary[13] in discussing four-level double resonance, the population n_i in the ith level is expressed in terms of the equilibrium population, n_i^0, and the deviation from it, δn_i, i.e., $n_i = n_i^0 + \delta n_i$. We also consider the velocity dependence $n_i(\beta)$ with $\beta = v/c$, such that $n_i(\beta)d\beta$ is the number of molecules in the ith level with a velocity component (in the z direction) between β and $\beta + d\beta$. Then at an electric field E, the change of molecular population δn brought about by the pumping is given by using the Karplus–Schwinger formula[14] to be

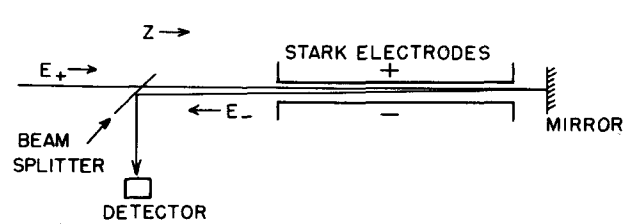

FIG. 2. A schematic representation of the experimental arrangement. The laser beam traverses a homogeneous dc electric field produced by the Stark electrodes in a cell containing the gas sample. It is then reflected by a mirror back through the Stark field and is directed by a beam splitter into the detector.

$$\frac{\delta n_4(\beta)}{n_2^0(\beta)} = -\frac{\delta n_2(\beta)}{n_2^0(\beta)}$$

$$= \frac{1}{2}\frac{(\mu_2 E_+/h)^2}{[\nu_1(1-\beta)-\nu_2(E)]^2+[\Delta\nu_2(\beta)]^2+(\mu_2 E_+/h)^2} \quad . \tag{6}$$

In Eq. (6), $\mu_2 E_+/h$ is the transition moment of the vibrational transition ν_2, which is typically 1 MHz under our experimental conditions, and $\Delta\nu_2(\beta)$ is the uncertainty broadening of the spectral line (with possible β dependence[15]) due to molecular and wall collisions and also due to limited transit time for the molecules in the laser field; this is estimated to be of the order of 0.2 MHz at our experimental pressures (≈ 5 mtorr). Under our conditions, Eq. (6) indicates that an appreciable number of molecules with a velocity such that $\nu_1(1-\beta) \approx \nu_2(E)$ are pumped from the ground level 2 to the excited level 4, and therefore a "hole" in the velocity profile of the ground state and a "spike" in the excited state are produced.[3] The pumped molecules then equilibrate with molecules in other levels and velocity states. For convenience, we adopt here the simplest thermalization model in which only the collision-induced transitions ϕ between levels 1 and 2, and 3 and 4, assumed to be equal, are considered. The vibrational transitions between 1 and 4, and 2 and 3, have much smaller probabilities and are neglected. All other collision-induced transitions are summarized as ξ transitions which connect the four levels in question with other levels which are regarded as the thermal bath. In contrast to the case of microwave double resonance, we must consider velocity changes accompanying collision-induced transitions. The rate of transitions from level 2 to level 1, or 4 to 3, changing the molecular velocity from β before the collision to β' after the collision is expressed as $k_\phi(\beta)\rho(\beta,\beta')$, where $\rho(\beta,\beta')$ is normalized such that

$$\int_{-\infty}^{\infty}\rho(\beta,\beta')d\beta' = 1 \quad . \tag{7}$$

The ∞ signs on the integral indicate infinity on v and not ultrarelativistic velocity. We use these here and hereafter in a purely mathematical sense. If the β' dependence of the ξ collisions is neglected, then we obtain the steady state equation

$$\frac{dn_i(\beta)}{dt} = \int_{-\infty}^{\infty} n_j(\beta')k_\phi(\beta')\rho(\beta',\beta)d\beta' + Nk_\xi(\beta) - n_i(\beta)[k_\phi(\beta)+k_\xi(\beta)] = 0 \quad , \tag{8}$$

where $(i,j) = (1,2)$ or $(3,4)$, and N is the total number of molecules excluding those in levels i and j. Subtracting the expression for thermal equilibrium [which is Eq. (8) in the absence of pumping] from Eq. (8), we obtain

$$\int_{-\infty}^{\infty}\delta n_j(\beta')k_\phi(\beta')\rho(\beta',\beta)d\beta' - \delta n_i(\beta)[k_\phi(\beta)+k_\xi(\beta)] = 0$$

if the small change in N with pumping is neglected. Therefore, we see that the population difference transferred from level 2 to level 1, or 4 to 3, is given by

$$\delta n_i(\beta) = [k_\phi(\beta)+k_\xi(\beta)]^{-1}\int_{-\infty}^{\infty}\delta n_j(\beta')k_\phi(\beta')\rho(\beta',\beta)d\beta' \quad . \tag{9}$$

Now we consider the absorption of the "signal" radiation E_-. Under our experimental conditions, the gas pressure is sufficiently low that the absorption is linearly proportional to the absorption coefficient γ. Therefore the *change* of absorption coefficient due to the collisionally transferred population changes $\delta n_1(\beta)$ and $\delta n_3(\beta)$ may be expressed as

$$\Delta I(E,\beta) = \frac{8\pi^2\nu_1\mu_1^2\Delta\nu_1(\beta)[\delta n_1(\beta)-\delta n_3(\beta)]}{3ch\{[\nu_1(1+\beta)-\nu_1(E)]^2+[\Delta\nu_1(\beta)]^2+(\mu_1 E_-/h)^2\}} \quad , \tag{10}$$

where μ_1 is the dipole transition moment for the vibration–rotation transition ν_1. The total change I_m of the absorption coefficient due to pumping is obtained by combining Eqs. (6), (9), and (10) and using the Maxwellian velocity distribution

$$n_2^0(\beta) = n_2^0(mc^2/2\pi kT)^{1/2}\exp(-mc^2\beta^2/2kT) \tag{11}$$

where n_2^0 is the total number of molecules in the level 2 at thermal equilibrium. We have

$$I_m(E) = \int_{-\infty}^{\infty}\Delta I(E,\beta)d\beta = -\frac{8\pi^2\nu_1\mu_1^2\mu_2^2E_+^2n_2^0}{3ch^3}\left(\frac{mc^2}{2\pi kT}\right)^{1/2}\int_{-\infty}^{\infty}\int_{-\infty}^{\infty}\left(\frac{k_\phi(\beta')\rho(\beta',\beta)}{k_\phi(\beta)+k_\xi(\beta)}\right) \times \Delta\nu_1(\beta)\exp\left(\frac{-mc^2\beta^2}{2kT}\right)\left\{[\nu_1(1+\beta)-\nu_1(E)]^2+[\Delta\nu_1(\beta)]^2+\left(\frac{\mu_1E_-}{h}\right)^2\right\}^{-1}\left\{[\nu_1(1-\beta')-\nu_2(E)]^2+[\Delta\nu_2(\beta')]^2+\left(\frac{\mu_2E_+}{h}\right)^2\right\}^{-1}d\beta d\beta' \quad . \tag{12}$$

It should be remembered that $I_m(E)$ in Eq. (12) represents the intensity of the double resonance signal, that is, the *variation* of the absorption coefficient due to the pumping with the E_+ radiation, and not the total absorption coefficient. The result of Eq. (12) gives collision-induced Lamb dips associated with molecules with positive v_m. There is another contribution from molecules with negative v_m in which E_+ pumps the ν_1 transition and E_- monitors the ν_2 transitions for which the expression of $I_m(E)$ is obtained by interchanging suffices 1 and 2 in Eq. (12). Since $\nu_1 \approx \nu_2$, $\Delta\nu_1 \approx \Delta\nu_2$, and $n_1^0 \approx n_2^0$, Eq. (12) is symmetric to 1 and 2 except for μ_1 and μ_2 in the denominators. For large M values we can approximate $\mu_1 \approx \mu_2$; then the two contributions just mentioned are equal in magnitude and the value of $I_m(E)$ is doubled.

In the preceding material, it has been assumed that the "probe" radiation, E_-, is sufficiently weak that it does not significantly affect the populations of levels 1 and 3. If the pump and probe radiations have similar intensities then $I_m(E)$ is given by the sum of two terms, the first as given in Eq. (12) and the second term the

same except for the interchange of subscripts 1 and 2 and subscripts + and −. This in effect adds to the expression for the absorption coefficient I_m a term which has E_-^2 instead of E_+^2 in the factor in front of the integral in Eq. (12).

The Lorentzian expressions in the integral of Eq. (12) are rapidly varying functions of β and β' but $k(\beta)$, $\Delta\nu(\beta)$, and $\exp(-mc^2\beta^2/2kT)$ are slowly varying functions of β. Therefore we can approximate the latter as constants using their values with $\beta=\beta_m$. Dropping β_m for simplicity from $k(\beta_m)$ and $\Delta\nu(\beta_m)$, and including the additional terms due to negative v_m and strong E_- radiation, we obtain the expression of $I_m(E)$ as

$$I_m(E)=-\frac{16\pi^2\nu n\Delta\nu\mu_1^2\mu_2^2(E_+^2+E_-^2)}{3ch^3}\left(\frac{mc^2}{2\pi kT}\right)^{1/2}\times\frac{k_\phi}{k_\phi+k_t}\exp\left(\frac{-mc^2\beta_m^2}{2kT}\right)\times\int_{-\infty}^{\infty}\int_{-\infty}^{\infty}\rho(\beta',\beta)\times\left\{[\nu_t(1+\beta)-\nu_1(E)]^2+(\Delta\nu)^2+\left(\frac{\mu_1E_-}{h}\right)^2\right\}^{-1}\times\left\{[\nu_t(1-\beta')-\nu_2(E)]^2+(\Delta\nu)^2+\left(\frac{\mu_2E_+}{h}\right)^2\right\}^{-1}d\beta d\beta' \quad . \tag{13}$$

It should be noted that $E_+>E_-$ since E_- is the reflected laser field. When E_- is made much smaller than E_+ by the use of a partially reflecting mirror, only the term with E_+ remains; if E_+ is made small, E_- is also small and $I_m(E)$ vanishes.

C. Limiting cases

The integration in Eq. (13) cannot be done analytically if a general form for $\rho(\beta',\beta)$ is assumed. However, we can consider two simple limiting cases.

1. Case I

If the molecules change their rotational state without change in velocity, then $\rho(\beta',\beta)$ is given by

$$\rho(\beta',\beta)=\delta(\beta',\beta) \quad , \tag{14}$$

where $\delta(\beta',\beta)$ is the Dirac delta function.

Then by contour integration we may obtain for the integral

$$I(E)=\int_{-\infty}^{\infty}\{[\nu_t(1+\beta)-\nu_1(E)]^2+\Gamma_1^2\}^{-1}\times\{[\nu_t(1-\beta)-\nu_2(E)]^2+\Gamma_2^2\}^{-1}d\beta=\frac{1}{\nu_t}\frac{\Gamma_1+\Gamma_2}{\Gamma_1\Gamma_2}\frac{\pi}{[2\nu_t-\nu_1(E)-\nu_2(E)]^2+(\Gamma_1+\Gamma_2)^2} \quad , \tag{15}$$

where $\Gamma_1^2=(\Delta\nu)^2+(\mu_1E_-/h)^2$ and $\Gamma_2^2=(\Delta\nu)^2+(\mu_2E_+/h)^2$. Thus we have the intensity of the double resonance signal at resonance ($E=E_m$) of

$$I_m(E_m)=-\frac{16\pi^2n\Delta\nu\mu_1^2\mu_2^2(E_+^2+E_-^2)}{3ch^3}\left(\frac{\pi mc^2}{2kT}\right)^{1/2}\times\frac{k_\phi}{k_\phi+k_t}\frac{1}{\Gamma_1\Gamma_2(\Gamma_1+\Gamma_2)}\exp\left(\frac{-mc^2\beta_m^2}{2kT}\right) \tag{16}$$

and a line shape of

$$I_m(E)=I_m(E_m)\frac{(\Gamma_1+\Gamma_2)^2}{[2\nu_t-\nu_1(E)-\nu_2(E)]^2+(\Gamma_1+\Gamma_2)^2} \quad . \tag{17}$$

Equation (17) indicates a sharp resonance at a field $E=E_m$ [see Eq. (14)] with a width similar to those of the Lamb dips at E_1 and E_2.

2. Case II

If the velocities of the molecules change very much during the collisions which result in changes of rotational state (i.e., if the dependence of $\rho(\beta',\beta)$ on β-β' is much slower than those of the Lorentzian functions in Eq. (13)], then we can approximate $\rho(\beta',\beta)$ by

$$\rho(\beta',\beta)=\rho[\beta_1(E),\beta_2(E)] \quad , \tag{18}$$

where

$$\beta_1(E)=[\nu_1(E)-\nu_t]/\nu_t$$

and

$$\beta_2(E)=[\nu_t-\nu_2(E)]/\nu_t \quad .$$

Equation (13) is then simplified to

$$I_m(E)=I_m(E_m)\frac{(\Gamma_1+\Gamma_2)\pi}{\nu}\rho[\beta_1(E),\beta_2(E)]\times\exp\left[\frac{mc^2[\beta_m^2-\beta_2^2(E)]}{2kT}\right] \quad . \tag{19}$$

In contrast to Eq. (17), the sharp feature with a width of the order of Γ (the collision-induced dip) is lost in Eq. (19) and the line shape is governed by the shape of ρ.

D. Relative intensities

In our experiments, Case I seems to be close to what is observed, so we will compare the I_m in Case I with that of normal Lamb dips. The absorption coefficient for the normal Lamb dips may be obtained by using the same formalism as in Sec. II B to be

$$I_1=-\frac{8\pi^2n\Delta\nu\mu_1^4(E_+^2+E_-^2)}{3ch^3}\left(\frac{\pi mc^2}{2kT}\right)^{1/2}\frac{1}{\Gamma_1\Gamma_1'(\Gamma_1+\Gamma_1')} \quad , \tag{20}$$

where $\Gamma_1'=[(\Delta\nu)^2+(\mu_1E_+/h)^2]^{1/2}$, and similarly for I_2. Assuming that $n_1^0\approx n_2^0$, and that $\Gamma_1'\approx\Gamma_2$ and $\Gamma_2'\approx\Gamma_1$, we then find that

$$\frac{I_m}{(I_1I_2)^{1/2}}=\frac{2k_\phi}{k_\phi+k_t}\exp\left(\frac{-mc^2\beta_m^2}{2kT}\right)^2=\frac{2k_\phi}{k_\phi+k_t}\exp\left[-\left\{\frac{\nu_1(E_m)-\nu_2(E_m)}{2f}\right\}^2\right], \tag{21}$$

where f is the Doppler width,[16] $f=\nu/c(2kT/m)^{1/2}$. The implication of Eq. (21) is clear. The intensity of the center dip is reduced by two factors: (a) the ratio of the rate of dip transferring collisions ϕ to the total collision rate and (b) the frequency mismatch factor, which varies as a Gaussian with a width equal to twice the Doppler width. The result is essentially in agreement with that obtained by Brewer *et al.*[6] by using a density matrix formalism. If the gas pressure is sufficiently high that the effect of wall collisions is negli-

gible, then $I_m/(I_1I_2)^{1/2}$ is independent of pressure because both k_ϕ and k_t are proportional to pressure. However, if the gas pressure is low, then $I_m/(I_1I_2)^{1/2}$ will be affected since the relative values of k_ϕ and k_t are very different for molecular collisions and wall collisions. Wall collisions are "hard" collisions which do not obey selection rules; therefore $k_t \gg k_\phi$ and the value of $I_m/(I_1I_2)^{1/2}$ is reduced at very low pressures. A similar effect due to wall collisions occurs in microwave double resonance[13] at low pressures.

III. OBSERVED SPECTRA

As discussed in the preceding section, $\nu_1(E_m) - \nu_2(E_m)$ must be of the order of or smaller than twice the Doppler width in order to observe a center dip. Virtually all of the systems of collision-induced transitions which we have studied are between different M levels for the same J,K states. However, for H_2CO there was one (negative) example of a four-level system between different K values. The results of our observations are summarized here for various molecules. The observed values of E_m are accurate to about 0.01 kV/cm, but the observed values of $I_m/(I_1I_2)^{1/2}$ could have errors of the order of 30% (depending on the experimental conditions). However their variation between the various transitions and molecules studied enables us to draw some conclusions about the nature of collision-induced reorientation collisions. For all spectra shown except the lower trace in Fig. 6 the laser and Stark electric fields were perpendicular, giving rise to $\Delta M = \pm 1$ transitions.

A. NH_3

There is a close coincidence (270 MHz) between the 13–12 (v'–v'') $P(15)$ line of the CO laser[17] at 1775.259 cm^{-1} and a $^{14}NH_3$ absorption line, and the resulting laser Stark spectrum has been analyzed by Johns, McKellar, and Trombetti.[7] The NH_3 line is a $R(9)$ transition of the perpendicular ν_4 band, and the upper state of the transition is strongly perturbed due to Coriolis interaction between the ν_4 and $2\nu_2$ vibrations. The spectrum is shown in Fig. 3, where three-level center dips[9,11] are indicated with asterisks and collision-induced four-level dips are indicated with dots. It is evident that the three-level dips have intensities about equal to the geometric mean of the two Lamb dips giving rise to them, as predicted.[11] The four-level dips are much weaker; their measured intensities are listed in Table I. Note that as $\nu_1(E_m) - \nu_2(E_m)$ approaches twice the Doppler width, the center dips become very weak.

B. H_2CO

The CO laser Stark spectrum of the ν_2 band (C=O stretching vibration) of H_2CO has been analyzed in detail,[12] but Lamb dip spectra were not obtained at that time. Here we will discuss spectra arising from two H_2CO transitions, $Q(1)$ and $R(4)$, in order to illustrate the formation of collision-induced Lamb dips. Figure 4 shows part of the spectrum obtained with the 14–13 $P(16)$ line of the CO laser at 1746.304 cm^{-1}, which lies just 0.3 cm^{-1} above the H_2CO ν_2 band origin. The full spectrum obtained with this line, but without Lamb dips,

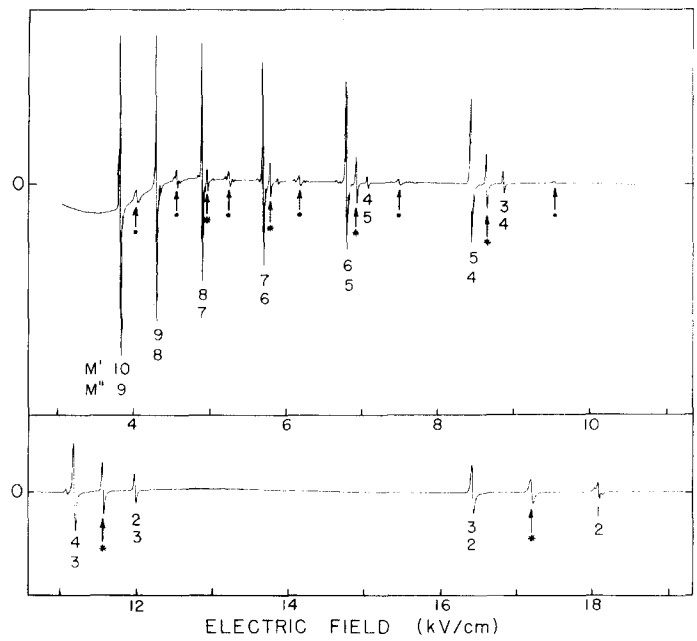

FIG. 3. Lamb dip Stark spectrum of NH_3 obtained with the 13–12 $P(15)$ line of the CO laser at 1775.259 cm^{-1}. This trace was obtained with an intracavity Stark cell having 3 mm plate spacing and with 10 mtorr pressure of NH_3. The lines indicated with arrows are center dips due to three-level (*) and four-level (·) double resonance effects.

is shown in Fig. 2 of Ref. 12. The Doppler profile of the spectrum in Fig. 4 shows that there are two partially overlapping lines, and each of these gives rise to a strong Lamb dip. In addition there is a weaker dip midway between the two strong dips; the energy level diagram in Fig. 5 illustrates the formation of the two lines, and shows that they indeed form an unambiguous four-level system in which the two transitions can be coupled only by collisions, in this case collisions involving $\Delta M = \pm 1$.

A portion of the spectrum obtained with the 14–13 $P(13)$ line of the CO laser at 1757.896 cm^{-1} is shown in Fig. 6. In the top spectrum, the electric field of the laser radiation was perpendicular to the Stark electric field, giving $\Delta M = \pm 1$ selection rules, and in the bottom spectrum the fields were oriented at about 45°, giving $\Delta M = 0$ transitions as well as $\Delta M = \pm 1$. The laser line lies close to the $R(4)$ transition of H_2CO, and lines involving $K_a = 3$ and 4 occur in the region covered by Fig. 6. The K_a, M', and M'' assignments of the lines are indicated in Fig. 6. All the observed Lamb dips occur near the center of a broad Doppler profile, and an idea of the scale can be obtained from the pair of lines with $K_a = 3$, $M' = 1$, and $M'' = 0$. The splitting between this pair of lines is almost exactly the asymmetry doubling of the $J = 4$, $K_a = 3$ level of the ground state of H_2CO, viz., 4.29 MHz. The much smaller splitting of the $K_a = 4$ doublet is not observed here since the linewidth is about 1 MHz. Weak center dips can be observed in the top spectrum of Fig. 6 between the two lines assigned to $K_a = 4$ and also between the $K_a = 3$ doublet and the other strong $K_a = 3$ line. The transitions which give

TABLE I. Observed center dips in NH_3 (Doppler width f = 96 MHz).

Transition	Collision-induced transitions[b] $M_4\ M_3$	$M_2\ M_1$	E_m (kV/cm)	$\nu_1-\nu_2$ (MHz)	$I_m/(I_1I_2)^{1/2}$
$^rR_3(9)$[a]	$\pm9\leftrightarrow\pm10$	$\pm8\leftrightarrow\pm9$	4.04	62	0.10
	$\pm8\cdot\cdot\pm9$	$\pm7\leftrightarrow\pm8$	4.57	71	0.13
	$\pm7\leftrightarrow\pm8$	$\pm6\leftrightarrow\pm7$	5.26	80	0.12
	$\pm6\cdot\cdot\pm7$	$\pm5\leftrightarrow\pm6$	6.19	94	0.12
	$\pm5\leftrightarrow\pm6$	$\pm4\cdot\cdot\pm5$	7.51	114	0.06
	$\pm4\leftrightarrow\pm5$	$\pm3\cdot\cdot\pm4$	9.58	145	0.02

[a]Refer to Ref. 7 for a detailed explanation of this NH_3 ν_4 band transition. The 13–12 ($v'\rightarrow v''$) $P(15)$ line of the CO laser at 1775.259 cm^{-1} was used for the observation.
[b]The subscripts on M refer to the numbering of levels in Fig. 1(c).

rise to the very weak pair of center dips at 10.83 kV/cm in the upper trace of Fig. 6 are illustrated in Fig. 7. The asymmetry splittings of the $M = 0$ levels are too small to be shown in Fig. 7. Note that the collisional transfers which cause the center dips in this case involve $\Delta M = 4$ in the lower state and $\Delta M = 6$ in the upper state. These large changes in M could either occur in a single collision, or sequentially over a number of collisions.

Note, however, that there are no center dips between lines with $K_a = 3$ and $K_a = 4$, even though they are separated by much less than the Doppler width. This is hardly surprising since it is known[1] that collisional transitions between ortho ($K_a = 3$) and para ($K_a = 4$) states are strongly forbidden. Stronger center dips can be observed in the lower spectrum of Fig. 6. There are three reasons why these dips are stronger: (1) the transitions are closer together ($\nu_1-\nu_2$ is smaller), (2) the collisional transitions which transfer the Lamb dips involve smaller changes in M, and (3) the energy separations of the levels connected by collisions are smaller. We believe that (2) is probably the most important of

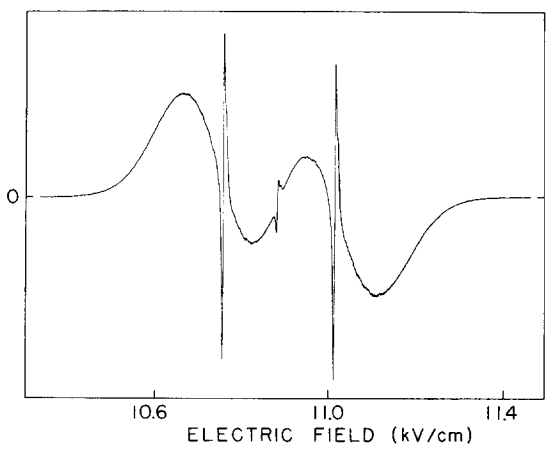

FIG. 4. Lamb dip Stark spectrum of H_2CO [the $^qQ_1(1)$ transition of the ν_2 band] obtained with the 14–13 $P(16)$ line of the CO laser at 1746.304 cm^{-1}. The two strong sharp features are the "real" Lamb dips, and the weaker sharp feature midway between them is the collisionally transfered center dip.

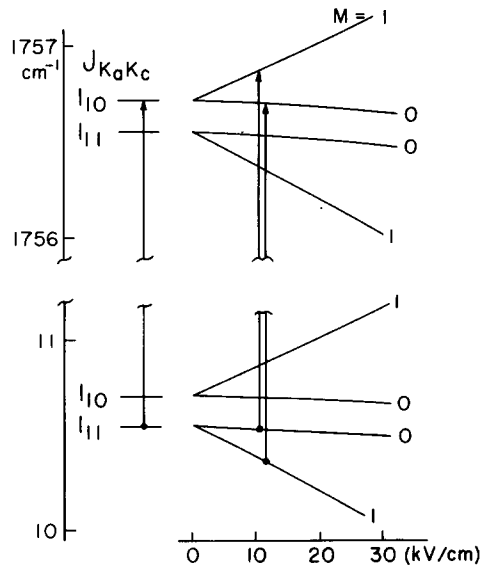

FIG. 5. Energy level diagram illustrating the $^qQ_1(1)$ transitions of H_2CO shown in Fig. 4. Note that the center dip arises from collision-induced transitions between the initial states, and between the final states, of these two transitions.

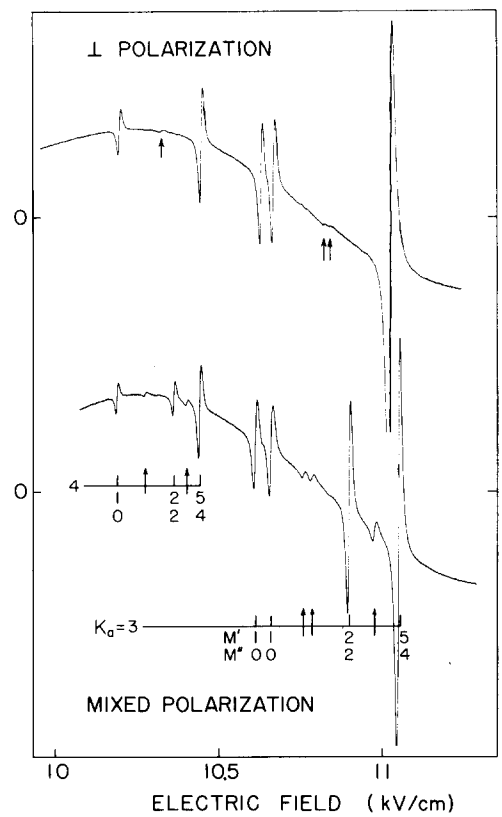

FIG. 6. Lamb dip Stark spectrum of H_2CO [$R(4)$ transitions of the ν_2 band] obtained with the 14–13 $P(13)$ line of the CO laser at 1757.896 cm^{-1}. The upper trace was taken with perpendicular polarization of the laser and Stark electric fields, giving rise to $\Delta M = \pm1$ selection rules, and the lower trace was taken with mixed polarization, giving $\Delta M = 0, \pm1$ transitions. The collision-induced center dips are indicated by arrows.

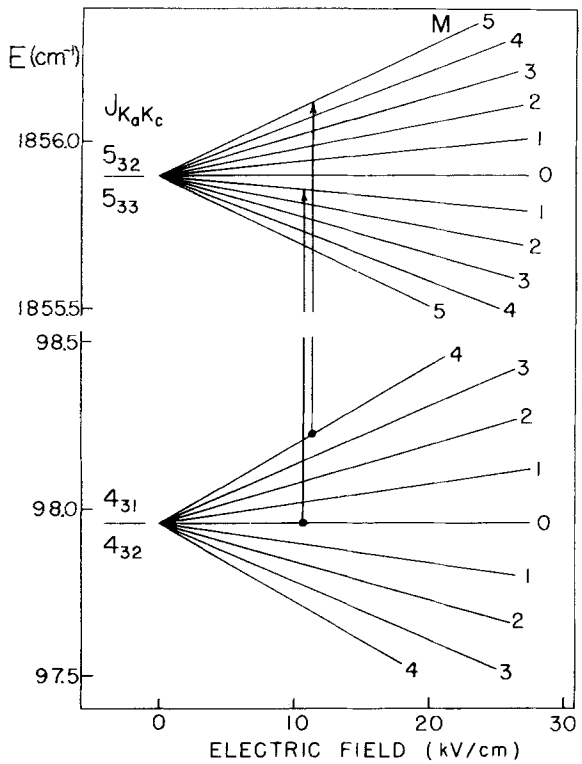

FIG. 7. Energy level diagram illustrating two of the $^qR_3(4)$ transitions shown in Fig. 6. The asymmetry doubling of the upper and lower states is too small to be shown on this scale. Note that the center dip between these two transitions arises from collision-induced transitions with $\Delta M = 4$ in the lower state and $\Delta M = 6$ in the upper state.

these. The measured resonant fields and intensities of the H_2CO center dips shown in Figs. 4 and 6 are listed in Table II.

In the course of our study of the $^qQ_1(1)$ line in H_2CO (Fig. 4), we made some preliminary studies of the pressure dependence of the center dip intensity, $I_m/(I_1I_2)^{1/2}$. Over a range of about 2–25 mtorr, we found that the intensity remained approximately constant. This result tends to confirm the prediction made in Sec. II D.

TABLE II. Observed center dips in H_2CO (Doppler width $f = 71$ MHz).

Transition	Collision-induced transitions[c] $M_4\ M_3$	$M_2\ M_1$	E_m (kV/cm)	$\nu_1-\nu_2$ (MHz)	$I_m/(I_1I_2)^{1/2}$
$^qQ_1(1)$[a]	$0 \cdot\cdot \pm 1$	$\pm 1 \leftrightarrow 0$	10.89	104	0.17
$^qR_3(4)$[b]	$\pm 5 \cdot\cdot \mp 1$	$\pm 4 \leftrightarrow 0$	10.83	40	0.02
	$\pm 2 \leftrightarrow \pm 1$	$\pm 2 \leftrightarrow 0$	10.76	25	0.05
	$\pm 5 \cdot\cdot \pm 2$	$\pm 4 \leftrightarrow \pm 2$	10.96	15	0.06
$^qR_4(4)$[b]	$\pm 5 \cdot\cdot \mp 1$	$\pm 4 \leftrightarrow 0$	10.31	46	0.05
	$\pm 2 \leftrightarrow \pm 1$	$\pm 2 \leftrightarrow 0$	10.27	31	0.12
	$\pm 5 \leftrightarrow \pm 2$	$\pm 4 \leftrightarrow 2$	10.40	15	0.10

[a]The 14–13 $P(16)$ line of the CO laser at 1746.304 cm^{-1} was used for this transition.
[b]The 14–13 $P(13)$ line of the CO laser at 1757.896 cm^{-1} was used for this transition.
[c]The subscripts on M refer to the numbering of levels in Fig. 1(c).

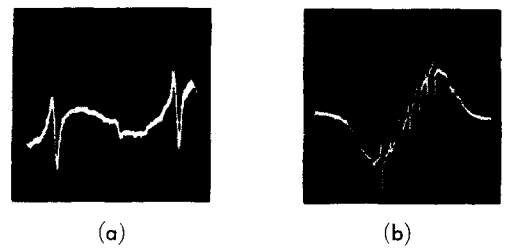

FIG. 8. Oscilloscope traces of the Lamb dip Stark spectrum of CH_3F (the ν_3 band) obtained with lines of the 9.4 μm band of the CO_2 laser. (a) is the $^qQ_1(1)$ transition of $^{12}CH_3F$ obtained with the $P(18)$ laser line at 1048.661 cm^{-1}, and (b) is the $^qQ_2(2)$ transition of $^{13}CH_3F$ obtained with the $P(40)$ laser line at 1027.382 cm^{-1}. In (b) the stronger four lines are the normal Lamb dips; note the relatively large intensity of the three center dips.

C. CH_3F

The CO_2 laser Stark spectra[8] of the ν_3 bands (C–F stretching vibration) of $^{12}CH_3F$ and $^{13}CH_3F$ provide several Q-branch transitions which demonstrate large center dips. Some of these are illustrated in Fig. 8, and the results are summarized in Table III. Compared with NH_3 and H_2CO, the intensities $[I_m/(I_1I_2)^{1/2}]$ measured for the CH_3F center dips are very large. Reasons for this are discussed in Sec. IV. In fact, for the $^qQ_2(2)$ lines of $^{13}CH_3F$, the intensities of the center dips are more than half of those of normal Lamb dips. Since the collision-induced transitions ξ which connect the levels in question with the thermal bath include at least one ϕ type transition, Eq. (21) predicts that the value of $I_m/(I_1I_2)^{1/2}$ cannot be greater than 1. The observed value of 0.6 indicates a large value for k_ϕ. If

TABLE III. Observed center dips in CH_3F (Doppler width $f = 40.2$ MHz for $^{12}CH_3F$, 38.8 MHz for $^{13}CH_3F$).

Transition	Collision-induced transitions[c] $M_3\ M_2$	$M_2\ M_1$	E_m (kV/cm)	$\nu_1-\nu_2$ (MHz)	$I_m/(I_1I_2)$
$^{12}CH_3F$[a]					
$^qQ_1(1)$	$0 \cdot\cdot \mp 1$	$\pm 1 \leftrightarrow 0$	4.509	71.1	0.33
$^{13}CH_3F$[b]					
$^qQ_1(1)$	$\pm 1 \cdot\cdot 0$	$0 \leftrightarrow \mp 1$	5.737	36.4	0.52
$^qQ_2(2)$	$\pm 2 \cdot\cdot \pm 1$	$\pm 1 \cdot\cdot 0$	4.747	32.1	0.57
	$\pm 1 \cdot\cdot 0$	$0 \cdot\cdot \mp 1$	4.852	32.9	0.61
	$0 \cdot\cdot \mp 1$	$\mp 1 \cdot\cdot \mp 2$	4.958	33.7	0.65
$^qQ_3(3)$	$\mp 3 \leftrightarrow \mp 2$	$\mp 2 \leftrightarrow \mp 1$	0.943	5.5	0.65
	$\mp 2 \leftrightarrow \mp 1$	$\mp 1 \cdot\cdot 0$	0.966	5.6	0.39
	$\mp 1 \cdot\cdot 0$	$0 \cdot\cdot \mp 1$	0.989	5.7	0.48
	$\mp 0 \cdot\cdot \pm 1$	$\pm 1 \leftrightarrow \pm 2$	1.010	5.9	0.47
	$\pm 1 \cdot\cdot \pm 2$	$\pm 2 \cdot\cdot \pm 3$	1.036	6.0	0.39
$^qQ_2(3)$	$\mp 3 \leftrightarrow \mp 2$	$\mp 2 \cdot\cdot \mp 1$	2.367	8.6	0.68
	$\mp 2 \cdot\cdot \mp 1$	$\mp 1 \cdot\cdot 0$	2.421	8.8	0.70
	$\mp 1 \cdot\cdot 0$	$0 \cdot\cdot \pm 1$	2.475	9.0	0.73
	$0 \leftrightarrow \pm 1$	$\pm 1 \cdot\cdot \pm 2$	2.535	9.3	0.78
	$\pm 1 \leftrightarrow \pm 2$	$\pm 2 \cdot\cdot \pm 3$	2.595	9.5	0.66

[a]The $P(18)$ line of the CO_2 laser at 1048.6608 cm^{-1} was used for the observation.
[b]The $P(40)$ line of the CO_2 laser at 1027.3822 cm^{-1} was used for the observation.
[c]The subscripts on M refer to the numbering of levels in Fig. 1(c).

the ϕ transitions are strongly allowed, as in this case, then the simple collisional model adopted in the derivation of Eq. (21) may not be a good approximation. The pumping of one M level by the laser will affect all the other M levels by the efficient ϕ transitions. Thus a steady state situation will arise in which all the M levels have burnt holes, and the velocity dependency of Nk_t in Eq. (8) cannot be ignored.

IV. DISCUSSION

The experimental results for NH_3, H_2CO, and CH_3F summarized in Tables I–III can be analyzed by using Eq. (21) to give values of $k_\phi/(k_\phi+k_t)$. These values give the relative importance of the reorientation transition ϕ, i.e., transitions in which the total angular momentum of the molecule changes its orientation with respect to space without changing its magnitude. Table IV summarizes the values of $k_\phi/(k_\phi+k_t)$ for various molecules and transitions. Since the relative intensity of the center dip depends on various experimental conditions such as laser power, modulation voltage, gas pressure, optical alignment, etc., and we have not completely studied the dependence, the values of $k_\phi/(k_\phi+k_t)$ have rather large uncertainties of the order of 30%. The values of $k_\phi/(k_\phi+k_t)$ in Table IV give us an insight into the nature and importance of the reorientation collisions ϕ.

A. Parity selection rules

Microwave double resonance experiments have shown[1] that, for polar molecules, collision-induced transitions following dipole selection rules are preferred to other collision-induced transitions, and specifically that parity-changing transitions $+ \leftrightarrow -$, are preferred over parity-conserving transitions $+ \leftrightarrow +$ or $- \leftrightarrow -$. Levels of CH_3F with $K \neq 0$ are doubly degenerate with double parity (+ and −), whereas those of NH_3 and H_2CO have a single parity (+ or −) at zero field. Therefore at zero electric field, the $\Delta M = \pm 1$ transitions are dipole allowed for CH_3F but forbidden for NH_3 and H_2CO. The larger values of $k_\phi/(k_\phi+k_t)$ for the CH_3F $\Delta M = \pm 1$ transitions compared to those for NH_3 and H_2CO are explained on this basis. When an electric field is applied the levels of the latter two molecules start to have mixed parity and transitions with $\Delta M = \pm 1$ become dipole allowed. In the limit of high field, that is, fields for which the Stark energy is considerably larger than the inversion doubling (for NH_3) or the asymmetry doubling (for H_2CO), the $\Delta M = \pm 1$ transitions are fully dipole allowed. The $^qQ_1(1)$ transition of H_2CO is an intermediate case for which the $M = \pm 1$ levels are shifted by an amount comparable to the asymmetry doubling and have mixed parity whereas the $M = 0$ levels are not much shifted and are still of nearly single parity. The observed NH_3 transition is in the weak field region where inversion splitting is much greater than the Stark shift. This explains the large value of $k_\phi/(k_\phi+k_t)$ for H_2CO, compared to NH_3, listed in Table IV.

TABLE IV. Observed values of $k_\phi/(k_\phi+k_t)$.

Molecule	Transition $(J', K') \leftarrow (J'', K'')$	Collision-induced transitions	$k_\phi/(k_\phi+k_t)$[a]
NH_3	(10, 10) ← (9, 9)	$\Delta M = \pm 1$	0.066
H_2CO	(1, 1) ← (1, 1)	$\Delta M = \pm 1$	0.143
	(5, 3) ← (4, 3)	$\Delta M = \pm 2, \pm 3$	0.026
		$\Delta M = \pm 4, \pm 6$	0.010
	(5, 4) ← (4, 4)	$\Delta M = \pm 2, \pm 3$	0.066
		$\Delta M = \pm 4, \pm 6$	0.026
$^{12}CH_3F$	(1, 1) ← (1, 1)	$\Delta M = \pm 1$	0.36
$^{13}CH_3F$	(1, 1) ← (1, 1)	$\Delta M = \pm 1$	0.32
	(2, 2) ← (2, 2)	$\Delta M = \pm 1$	0.37
	(3, 3) ← (3, 3)	$\Delta M = \pm 1$	0.36
	(3, 2) ← (3, 2)	$\Delta M = \pm 1$	0.23

[a]The uncertainties of these values are about 30%.

B. ΔM selection rules

The results for H_2CO listed in Table IV indicate that the values of k_ϕ are smaller for reorientation transitions with larger ΔM. In the treatment given in Sec. II, we ignored cascading type transitions because we considered only the four levels directly involved and treated the rest as the thermal bath. In the system where $\Delta M \neq 0$ transitions are allowed very efficiently, this may not be a good approximation and a higher order treatment such as that given in Ref. 13 may be needed. However the results in Table IV suggest that the $\Delta M > 1$ signals are caused mostly by single transitions. If they were the result of cascading, the value of $k_\phi/(k_\phi+k_t)$ for the $\Delta M = \pm 4$, ± 6 signals would be approximately equal to the square of the value for the $\Delta M = \pm 2$, ± 3 signals. The results therefore indicate that large reorientations ($\Delta M > 1$) of the total angular momentum can occur without changing the magnitude of J and without appreciable velocity change.

This may be explained by considering higher order dipole–dipole interactions for the resonant case, i.e., the case for which the total rotational energy does not change during the collision, as described in Sec. II. D. of Ref. 1. When the dipole–dipole interaction is assumed, the probability as a function of time for the $\Delta M = \pm 1$, $\Delta J = 0$ transition is

$$P_{M,M\pm1}(t) = \left|\frac{1}{\hbar}\int_{-\infty}^{t} \langle \alpha, M \left| V(t') \right| \alpha', M \pm 1 \rangle dt' \right|^2 , \quad (22)$$

where α summarizes all the quantum numbers other than M. Equation (22) indicates that it takes a time of about

$$t \approx \left| \langle \alpha, M \left| V(t') \right| \alpha', M \pm 1 \rangle / \hbar \right|^{-1} \sim 3\hbar r^3/\mu^2 \quad (23)$$

to "complete" a $\Delta M = \pm 1$ transition during a collision, where the factor 3 is introduced to account for the direction cosine. For H_2CO ($\mu = 2.33$ D) molecules at a distance of $r = 10$ Å, t is estimated to be of the order of 0.6 psec. Therefore if a collision lasts for $t \approx r/v \approx 3$ psec, there is sufficient time to complete several $\Delta M = \pm 1$ transitions during an encounter.

C. The k_ϕ transitions

The large values of $k_\phi/(k_\phi+k_\ell)$ for CH_3F and the consideration of other results just given indicate that the reorientation transitions have large probabilities. Since k_ℓ includes at least one k_ϕ transition the value of $k_\phi/(k_\phi+k_\ell)$ of 0.35 as observed in CH_3F demonstrates that the ratio of reorienting transitions ($\Delta M = \pm 1$, $\Delta J = 0$) to other transitions is at least 70%. If we include $|\Delta M| > 1$ transitions this number will be even larger.

For NH_3 and H_2CO at zero electric field the probability of $\Delta M = \pm 1$ (parity $+ \leftrightarrow +$, $- \leftrightarrow -$) transitions is lower because of the parity rule as shown by mircowave double resonance experiments (see Sec. III. C. 4 of Ref. 1). For these molecules $\Delta M = \pm 1$ ($+ \leftrightarrow +$, $- \leftrightarrow -$) transitions are caused mostly as the second-order process of $\Delta M = \pm 1$ ($+ \leftrightarrow -$) and $\Delta M = 0$ ($+ \leftrightarrow -$). It will be an interesting experiment to observe $\Delta M = \pm 2$ transitions in NH_3 or H_2CO at low field. They should have a probability similar to $\Delta M = \pm 1$. If the field is very high, there should not be much difference between NH_3 and CH_3F, because the former is no longer inverting.

D. Velocity changes

The observation of sharp center dips confirms our earlier conclusion in Ref. 3 that molecules may change their quantum state with only very small changes in their velocity. The collisions studied here are very subtle encounters with a large intermolecular distance (say 20 Å) so that the long-range dipole–dipole interaction can apply enough torque to reorient the molecules but does not change the molecular path appreciably.

The change of velocity due to dipole–dipole interaction can be estimated by a classical model. The force exerted between two dipoles separated by a distance r is

$$F = -\partial V/\partial r \approx \mu^2/r^4 , \tag{24}$$

where again a factor of 3 is assumed to account for the direction cosine. The force could be attractive or repulsive depending on the mutual orientation of the colliding molecules. The change of linear momentum of a molecule due to the force which is exerted during a collision for a time of $t \approx r/v$ is therefore estimated to be μ^2/vr^3. If we compare this with the average linear momentum mv at thermal velocities, we find the fractional change of linear momentum, and hence velocity, to be μ^2/mv^2r^3. This value for molecules with a dipole moment of 2D is typically 0.01 for $r = 20$ Å.

It will be very interesting to monitor the linewidths more carefully to detect a difference between the normal Lamb dips and collision-induced center dips. Such a difference is expected because of the small deflection of the molecular path due to collisions.[4,18] An appreciable velocity change is expected especially for the harder collisions which occur for nonpolar collision partners. As has been pointed out in Ref. 3, the advantage of four-level infrared–infrared double resonance compared to conventional microwave double resonance is that it can provide information on velocity changes at the same time as information on the selection rules governing changes in rotational state.

ACKNOWLEDGMENTS

We are grateful to Dr. A. E. Douglas for his critical reading of the manuscript and to Dr. U. Andresen for his help with some of the measurements on CH_3F.

*Presented at the 29th Symposium on Molecular Structure and Spectroscopy, Columbus, Ohio, 10–14 June 1974, and the Canadian Association of Physicists Annual Congress, St. John's, Newfoundland, 10–13 June 1974.

†Holder of a German Academic Exchange Service Fellowship. Present address: Abteilung für Physikalische Chemie, Universität Ulm, Ulm, Germany.

[1]For a summary, see T. Oka, Adv. At. Mol. Phys. 9, 127 (1973).
[2]T. Shimizu and T. Oka, Phys. Rev. A 2, 1177 (1970).
[3]S. M. Freund, J. W. C. Johns, A. R. W. McKellar, and T. Oka, J. Chem. Phys. 59, 3445 (1973).
[4]T. W. Meyer and C. K. Rhodes, Phys. Rev. Lett. 32, 637 (1974).
[5]R. G. Brewer, M. J. Kelly, and A. Javan, Phys. Rev. Lett. 23, 559 (1969).
[6]R. G. Brewer, R. L. Shoemaker, and S. Stenholm, Phys. Rev. Lett. 33, 63 (1974); R. L. Shoemaker, S. Stenholm, and R. G. Brewer, Phys. Rev. A 10, 2037 (1974).
[7]J. W. C. Johns, A. R. W. McKellar, and A. Trombetti, J. Mol. Spectrosc. (to be published).
[8]S. M. Freund, G. Duxbury, M. Römheld, J. T. Tiedje, and T. Oka, J. Mol. Spectrosc. 52, 38 (1974).
[9]E. E. Uzgiris, J. L. Hall, and R. L. Barger, Phys. Rev. Lett. 26, 289 (1971); see also T. W. Hänsch, I. S. Shahin, and A. L. Schawlow, *ibid.* 27, 707 (1971).
[10]W. Kreiner and T. Oka (private communication).
[11]H. R. Schlossberg and A. Javan, Phys. Rev. 150, 267 (1966).
[12]J. W. C. Johns and A. R. W. McKellar, J. Mol. Spectrosc. 48, 354 (1973).
[13]T. Oka, J. Chem. Phys. 47, 13 (1967).
[14]R. Karplus and J. Schwinger, Phys. Rev. 73, 1020 (1948).
[15]A. T. Mattick, A. Sanchez, N. A. Kurnit, and A. Javan, Appl. Phys. Lett. 23, 675 (1973).
[16]The usual spectroscopic definition of Doppler width is the precise half-width at half-height and is given by the quantity f multiplied by $(\ln 2)^{1/2}$.
[17]The CO laser wavenumbers are calculated from the constants given by H. Kildal, R. S. Eng, and A. H. M. Ross, J. Mol. Spectrosc. 53, 479 (1974).
[18]J. Schmidt, P. R. Berman, and R. G. Brewer, Phys. Rev. Lett. 31, 1103 (1973).